

Fast Dynamical Evolution of Hadron Resonance Gas via Hagedorn States

M Beitel, K Gallmeister and C Greiner

Institut für Theoretische Physik, Goethe-Universität Frankfurt am Main,
Max-von-Laue-Str. 1, 60438 Frankfurt am Main, Germany

E-mail: gallmeister@th.physik.uni-frankfurt.de

Abstract. Hagedorn states (HS) are a tool to model the hadronization process which occurs in the phase transition region between the quark gluon plasma (QGP) and the hadron resonance gas (HRG). These states are believed to appear near the Hagedorn temperature T_H which in our understanding equals the critical temperature T_c . A covariantly formulated bootstrap equation is solved to generate the zoo of these particles characterized baryon number B , strangeness S and electric charge Q . These hadron-like resonances are characterized by being very massive and by not being limited to quantum numbers of known hadrons. All hadronic properties like masses, spectral functions etc. are taken from the hadronic transport model Ultra Relativistic Quantum Molecular Dynamics (UrQMD). Decay chains of single Hagedorn states provide a well description of experimentally observed multiplicity ratios of strange and multi-strange particles as the Ξ^0 - and the Ω^- -baryon. In addition, the final energy spectra of resulting hadrons show a thermal-like distribution with the characteristic Hagedorn temperature T_H . Box calculations including these Hagedorn states are performed. Indeed, the time scales leading to equilibration of the system are drastically reduced down to $2 \dots 5 \text{ fm}/c$.

1. Introduction

Back in the 60's of the last century and before the advent of quantum chromodynamics (QCD) as the theory of strong interactions, R. Hagedorn [1] proposed the existence of a whole zoo of massive, unobserved hadronic resonance states. The spectrum of these particles, known as Hagedorn spectrum, exhibits the specific feature of being exponential in the infinite mass limit with the slope given by the so called Hagedorn temperature T_H . This temperature denotes the limiting temperature for hadronic matter since any partition function of a HRG with Hagedorn-like mass spectrum diverges as long as $T > T_H$. Above the Hagedorn temperature a new state of matter, namely the QGP, shall be realized. Thus, Hagedorn states provide a tool to understand the phase transition from HRG to QGP and back. The Hagedorn states are created in multi-particle collisions most abundantly near T_H which in our understanding equals to the critical temperature T_c . Hagedorn states are color neutral objects which are allowed to have any quantum numbers as long as they are compatible with its mass. The appearance of Hagedorn states in multi-particle collisions and their role was already discussed in [2, 3, 4, 5, 6]. Their appearance near T_c can explain, as shown in [4, 5, 6], the fast chemical equilibration of (multi-) strange baryons B and their anti-particles \bar{B} at Relativistic Heavy Ion Collider (RHIC) energies. The inclusion of Hagedorn states in a hadron resonance gas model provides also a lowering of

the speed of sound, c_s and of the shear viscosity over entropy density ratio η/s at the phase transition and being in good agreement with lattice calculations [7, 8, 9, 10].

2. Model and Results

The starting point of all calculations provided here is the postulate of the statistical bootstrap model (SBM) stating that fireballs consist of fireballs which in turn consist of fireballs etc. . As shown in [11] (cf. also [12]) the mathematical formulation of this postulate in the formulation of [13, 14] leads to the evolving bootstrap equation for the density of states,

$$\begin{aligned} \tau_{\vec{C}}(m) = & \frac{R^3}{3\pi m} \sum_{\vec{C}_1, \vec{C}_2} \int_{m_1^0}^m dm_1 m_1 \tau_{\vec{C}_1}(m_1) \int_{m_2^0}^{m-m_1} dm_2 m_2 \tau_{\vec{C}_2}(m_2) \\ & \times p_{\text{cm}}(m, m_1, m_2) \delta^{(3)}(\vec{C} - \vec{C}_1 - \vec{C}_2), \end{aligned} \quad (1)$$

where the conservation of the quantum numbers baryon number, strangeness and electrical charge $\vec{C} = (B, S, Q)$ is guaranteed. A major aspect was to restrict on Hagedorn states, which just consist of two constituents in order to allow for generation processes as $2 \rightarrow 1$ and decay as $1 \rightarrow 2$. This is some necessary constraint in order to allow for a microscopical calculation in a transport model simulation based on cross sections. The above set of integral equations of Volterra type is solved numerically by discretizing the mass range and consecutively stepping to higher mass bins. The zeroth order input are the known hadrons according their spectral functions as implemented in the transport model UrQMD [15].

The radius R is the only free parameter of the model. Choosing reasonable values as $R = 0.8 \text{ fm}$ (1.0 fm) yield Hagedorn temperatures, i.e. the slopes of the exponentially rising Hagedorn spectra $\tau_{\vec{C}}(m) \sim m^a \exp(m/T_H)$ as $T_H = 162 \text{ MeV}$ (145 MeV) nearly independent of the quantum numbers, as indicated in fig. 1.

In order to treat the decay and the production of Hagedorn states, the decay width Γ and the production cross section $\sigma = \pi R^2$ are connected via detailed balance as

$$\begin{aligned} \Gamma_{\vec{C}}(m) = & \frac{\sigma}{2\pi^2 \tau_{\vec{C}}(m)} \sum_{\vec{C}_1, \vec{C}_2} \int_{m_1^0}^m dm_1 \tau_{\vec{C}_1}(m_1) \int_{m_2^0}^{m-m_1} dm_2 \tau_{\vec{C}_2}(m_2) \\ & \times p_{\text{cm}}^2(m, m_1, m_2) \delta^{(3)}(\vec{C} - \vec{C}_1 - \vec{C}_2), \end{aligned} \quad (2)$$

which represents the second major equation of the model. Corresponding Hagedorn spectra and their decay width are shown in fig. 1. One observes, that the slope decreases with increasing volume of the Hagedorn state. Correspondingly also the width decreases. Nevertheless, for larger masses, the width is nearly constant in the range of some hundreds of MeV, and also stays finite in the infinite mass limit.

Having the total decay width and the corresponding composition, one is able to calculate the branching ratios for the decay into light Hagedorn states and/or hadrons. Performing such cascading decay simulations, the resulting hadron multiplicity coincide very well with experimentally observed value[11]. This is visualized in fig. 2, where the multiplicity ratios for strange and multi-strange particles are compared with experimental values measured at LHC. The most striking result is the fact, that the energy spectra of these decay hadrons *look* thermal, i.e. the functional behavior is exponential, as shown in fig. 2. The slope parameter coincides with the underlying Hagedorn temperature.

All these ingredients were implemented into UrQMD [15], which can handle the creation and the decay of Hagedorn states and their component dynamically. This enables us to perform box calculations and study the time evolution and the equilibration of the system. The model is able to handle different initialization scenarios, as e.g. the initialization with only nucleons (or

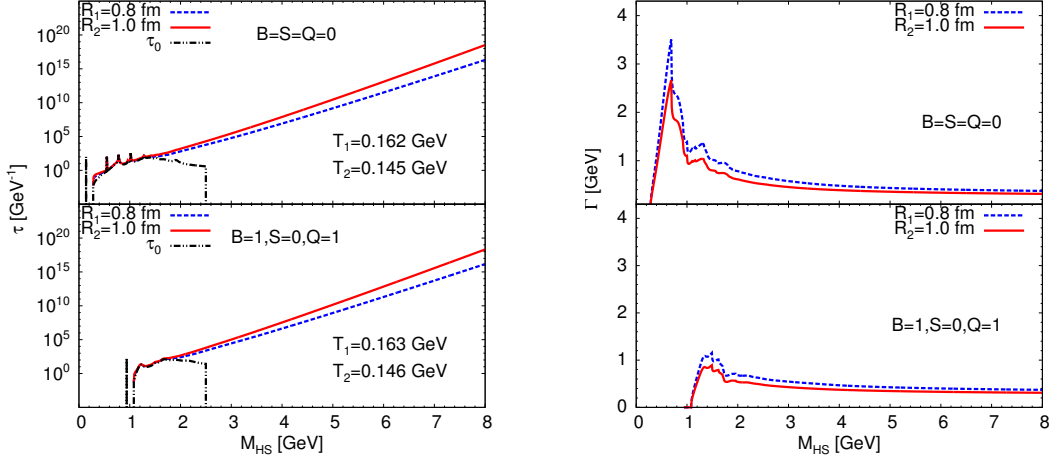


Figure 1. Hagedorn spectrum (left) and total decay width (right) for meson-like ($B = S = Q = 0$) (upper panel) and baryon-like ($B = 1, S = 0, Q = 1$) (lower panel) Hagedorn states. τ_0 denotes the sum of spectral functions of hadrons with the same quantum numbers.

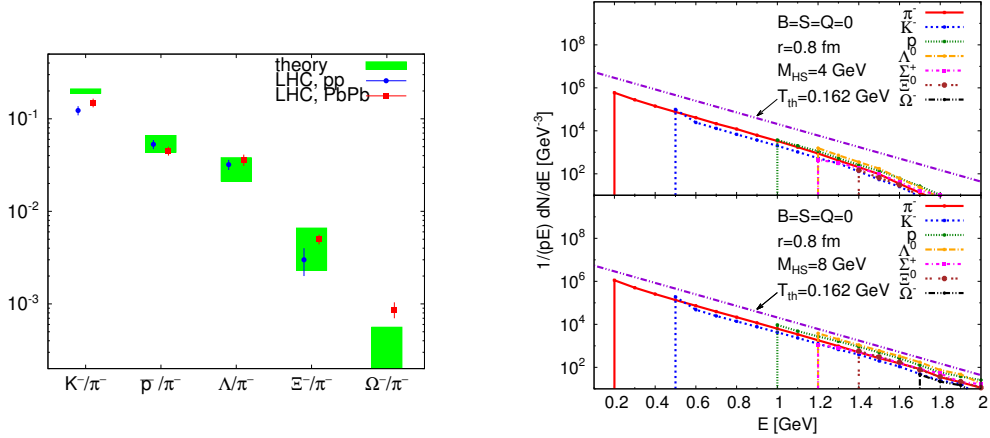


Figure 2. Left: Comparison of particle multiplicity ratios from theory vs. p-p at $\sqrt{s_{NN}} = 0.9$ TeV [16] and Pb-Pb at $\sqrt{s_{NN}} = 2.76$ TeV [17, 18, 19], both from ALICE at LHC. The bands show the range of calculations from cascade decay of a single charge neutral Hagedorn state with radius $R = 0.8$ fm and initial mass $M_{HS} = 4$ GeV and $M_{HS} = 8$ GeV. Right: Energy spectra of hadrons stemming from cascade decay of charge neutral Hagedorn state with radius $R = 0.8$ fm and initial mass $M_{HS} = 4$ GeV and $M_{HS} = 8$ GeV.

pions) with a given particle and energy density. While this may stand for some 'bottom-up' scenario, alternatively one may start with a given Hagedorn state distribution and look into the resulting hadron distributions. This indicates a 'top-down' scenario, where the Hagedorn states may stem from some preceding deconfined phase.

Fig. 3 shows the time dependence of Omega baryons for box calculations, where only Hagedorn states according to different energy densities were initialized. The given multiplicities at some time are the resulting multiplicities, if all particles would decay down to the stable remnants. One indeed observes very short time scales for the equilibration: For $t \leq 1 - 2$ fm/c the most hadrons have kinetically and chemically equilibrated. Even due to bad statistics for the multi-strange baryon Ω^- it is apparent that the chemical equilibration is established for $t = 5 - 10$ fm/c. In addition we find, that the energy spectra of the hadrons again

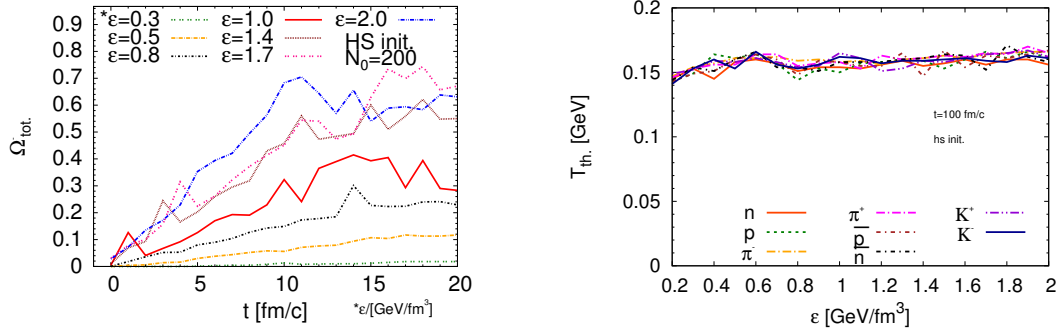


Figure 3. On the left the time dependence of Ω^- baryons in a box calculation is shown, initialized with Hagedorn states, for different initial energy densities as indicated in the plot. On the right the dependence of particle's Boltzmann slopes (temperatures) as function of energy density is depicted.

follow an exponential shape, with slope parameters very close to the Hagedorn temperature $T_H = 162 \text{ MeV}$, see fig. 3.

3. Conclusion

We conclude, that Hagedorn states are a valuable tool for the understanding of the phase transition between a deconfined and a hadronic phase. While already the decay particles of one single Hagedorn state *look* thermal with the Hagedorn temperature as the only scale, a collective system of Hagedorn states leads to small equilibration times of hadrons in the order of few fm/c. Even exotic multi-strange baryons as the Ω^- seem to equilibrate on such short time scales. These remarkable features may also open the door for alternative descriptions of heavy ion collisions, where directly from a pure gluonic phase without quarks a transition to the confined phase is possible [20].

- [1] Hagedorn R 1965 *Nuovo Cim. Suppl.* **3** 147–186
- [2] Greiner C and Leupold S 2001 *J. Phys. G* **27** L95–L102
- [3] Greiner C, Koch-Steinheimer P, Liu F M, Shovkovy I A and Stoecker H 2005 *J. Phys. G* **31** S725–S732
- [4] Noronha-Hostler J, Greiner C and Shovkovy I 2008 *Phys. Rev. Lett.* **100** 252301
- [5] Noronha-Hostler J, Greiner C and Shovkovy I 2010 *J. Phys. G* **37** 094017
- [6] Noronha-Hostler J, Beitel M, Greiner C and Shovkovy I 2010 *Phys. Rev. C* **81** 054909
- [7] Noronha-Hostler J, Noronha J and Greiner C 2009 *Phys. Rev. Lett.* **103** 172302
- [8] Majumder A and Muller B 2010 *Phys. Rev. Lett.* **105** 252002
- [9] Noronha-Hostler J, Noronha J and Greiner C 2012 *Phys. Rev. C* **86** 024913
- [10] Jakovac A 2013 *Phys. Rev. D* **88** 065012
- [11] Beitel M, Gallmeister K and Greiner C 2014 *Phys. Rev. C* **90** 045203
- [12] Yellin J 1973 *Nucl. Phys. B* **52** 583–594
- [13] Frautschi S C 1971 *Phys. Rev. D* **3** 2821–2834
- [14] Hamer C and Frautschi S C 1971 *Phys. Rev. D* **4** 2125–2137
- [15] Bass S A *et al.* 1998 *Prog. Part. Nucl. Phys.* **41** 255–369
- [16] Aamodt K *et al.* (ALICE) 2011 *Eur. Phys. J. C* **71** 1594
- [17] Abelev B *et al.* (ALICE Collaboration) 2013 *Phys. Rev. C* **88** 044910
- [18] Abelev B B *et al.* (ALICE Collaboration) 2013 *Phys. Rev. Lett.* **111** 222301
- [19] Abelev B B *et al.* (ALICE Collaboration) 2014 *Phys. Lett. B* **728** 216–227
- [20] Stoecker H *et al.* 2016 *J. Phys. G* **43** 015105